Multimedia Tools and Applications (2023) 82:12211–12227
https://doi.org/10.1007/s11042-022-13724-z

Deformable model segmentation for range image watermarking

Amine Khaldi [1] · Med Redouane Kafi [2] · Akram Zine Eddine Boukhamla [1]

Received: 7 April 2021 / Revised: 3 June 2022 / Accepted: 25 August 2022 /
Published online: 20 September 2022

Abstract
In this work, a range image watermarking approach is proposed. First, the image is segmented using active contours; the watermark is then integrated into the resulting contour coordinates. Three active contour methods are used to segment the range image, the obtained segmentation results allow to define the algorithm offering a good compromise between the good segmentation rate and the contour size which constitutes the watermark integration area. The imperceptibility and robustness tests performed show that the proposed scheme offers a good imperceptibility rate as well as a good structural similarity between the original and watermarked image. The watermark is resistant to several attacks commonly used in image watermarking, however, is vulnerable to compression attacks, which is common in spatial integration techniques.

Keywords Digital watermarking · Range image · Range segmentation · Active contour

1 Introduction

The networks and computer technology development allow the transmission of all kinds of text, sound and image information, which leads to easy and undetectable duplication and modification [20]. Despite the existence of protection techniques relating to the digital data

✉ Amine Khaldi
Khaldi.Amine@univ–ouargla.dz

Med Redouane Kafi
Kafi.Redouane@univ-ouargla.dz

Akram Zine Eddine Boukhamla
boukhamla.akram@univ-ouargla.dz

[1] Computer Science Department, Faculty of Sciences and Technology, Artificial Intelligence and Information Technology Laboratory (LINATI) University of Kasdi Merbah, 30000 Ouargla, Algeria

[2] Departments of Electronics, Faculty of Sciences and Technology, Electrical Engineering Laboratory, University of Kasdi Merbah, 30000 Ouargla, Algeria

transmission like cryptography, the content protection of a digital multimedia has yet been satisfactorily unresolved [15]. Among the first techniques that have been realized to guarantee security during the data transmission through a network remains cryptography [49], which allows to encrypt documents and ensure the security properties (confidentiality, integrity and authentication) and allows to secure the data only during its transmission [31] but after the decryption process the file is no longer protected and easily distributed by unauthorized users [24]. Watermarking has therefore been proposed to increase the sharing security by keeping the data confidentiality and checking the image integrity [21]. Image watermarking consists of inserting imperceptible and indelible information into the digital document to identify the copyright [3]. In addition to copyright protection, the application of watermarking techniques has been extended to other areas such as image indexing or image integrity control. Several techniques have already been proposed [35]; some approach consists in directly modifying the image pixels, others transform the image with a transform like DCT or DWT then the watermark is integrated in the coefficients obtained [39]. In some works, the image is segmented to integrate the watermark in the regions of interest [25]. In this work, we propose a range image watermarking approach. The image is segmented by active contour, and then the watermark is integrated into the coordinates of the resulting snake. Different range segmentation approaches have been proposed, these methods are similar to the methods used for conventional 2D image segmentation [1]. However, we noticed none of the authors have experimented or presented a range image watermarking method. In this work:

- Three active contour methods will be used to segment the range image and the watermarking results using the three different snakes will be compared.
- Objective similarity measurements will then be calculated to assess the imperceptibility of the integration process and the watermark robustness.

Because of unavailability of similar work, the results will be compared between the three proposed approaches. The document is organized as follows, the second section is dedicated to the watermarking and the range image presentation. The proposed watermarking approach and the three active contour segmentation algorithms will be presented in section 3. Experimental results as well as imperceptibility and robustness tests will be performed in section 4. The conclusion and perspective of this work will be presented in section 5.

2 Background

2.1 Digital watermarking

Image watermarking, as previously mentioned, represent a process of inserting a secondary signal into an image so that the signal can be detected or extracted later to represent an assertion on the image [30]. In general, any watermarking system consists of the following three parts:

- The watermark generation: The data insertion depends on the watermarking application. Some applications are based on including data such as inserting author's name, and others are based on inserting a significant part of a small image into a larger image [32]. Cryptography techniques based on the key to check if users have authorized access to

the data and also this key can be used in the watermarking system to generate randomly the signature [52].

- The insertion process that inserts the mark into the host media. The entries of the watermarking insertion are the mark, the original data and the security key [5]. The mark which can represent a sequence of numbers, a binary bit sequence or can represent an image [45]. The key is used to enhance the security of the watermarking system.
- The extraction process that extracts and confirms the presence of the mark. In the extraction process the entries are the watermarked data, the security key and the initial data and/or the original mark depending on the technique used [4]. If the extractor does not require the availability of the original image, the watermarking scheme is called "blind watermarking" [9]. If the extractor involves the initial image, it is considered "non-blind watermarking".

2.1.1 Watermarking system properties

The essential properties of a watermarking system are robustness, invisibility or imperceptibility and capacity [36]. There must be a compromise between the necessities and properties of watermarking according to its applications.

- Capacity: represent the amount of information inserted [10]. The current trend is to insert an amount of information at least equal to 64 bits.
- Imperceptibility: The watermark integration must not affect the quality of the initial image after the embedding process [33]. The watermark must be invisible to the human visual system. (HVS). The insertion process should not deteriorate the host image; the watermarked image should be visually equivalent to the original image [26].
- Robustness: The watermark should be robust enough to resist attacks and image manipulation. The algorithm must be robust to tolerate some changes in the image like compression, rotation or noise addition [2].

2.1.2 Different watermarking forms

According to its application, different types of watermarking can be used:

- Fragile watermarking: In the case of fragile or weak marking, imperceptibility must be significantly high and robustness very low [12]. Thus, the mark will not support any treatment, which allows to certify the image's integrity.
- Robust watermarking: This is the most widely used form of digital watermarking, it is generally invisible [50]. In this type, the visible watermarking is a logo but with a strong robustness.
- Symmetrical watermarking (private): Similar principle as in cryptography, symmetrical marking means that the same key is used to insert and detect the watermark [42].
- Asymmetrical watermarking: In this type of marking, the insertion key and the detection key are different [17]. The advantage is anyone can read the signature, without being able to extract or modify it.

2.1.3 Digital image watermarking applications

The digital watermarking applications are several, such as:

- Copyright protection; which was one of the first application of digital watermarking. In case of a legal dispute, the owner of an image is able to prove he is the owner even if the image has been modified [37].
- Content authentication of an image, which consists of inserting a fragile mark into an image that serves to alert the user to a possible modification of the image by an unauthorized person and precisely establish the manipulated regions [11]. This application is principally used in the legal and medical fields.
- Digital data can be duplicated without quality deterioration. In this context, if a person has a digital document and is malicious, he or she can illegally produce an unlimited number of copies of that document with a similar quality to the authentic document [23]. Digital watermarking can address this situation. Information about the number of copies allowed is encrypted in the mark [27]. This principle has been implemented in videos where the mark indicates whether the video can be copied or not.

2.2 Range segmentation

2.2.1 Range image

A range image is a two-dimensional array of 3D coordinates [34] that check the spatial coherence attribute. Each element of this matrix represents the distance between a reference point (in general the sensor itself) and a point in the field of view of the sensor (camera). It is the equivalent of a video image in which the grey level of each pixel (x, y) would be replaced by a z-altitude.

2.2.2 Range image acquisition

Range image sensors are used to collect 3D coordinates of reflective surfaces of objects in a scene; these sensors can be classified as either active or passive [19]. Active sensors project a signal onto a scene and measure the part of the signal reflected, radar, sonar and laser are examples of active sensors. Passive sensors operate using existing environmental conditions (a stereo airborne imaging system remain an excellent example).

2.2.3 Range image segmentation

The segmentation process is considered to represent likely the most essential step in image analysis as its performance directly affects the next processing steps of the image and significantly affects the interpretation of the resulting image [22]. The two principal difficulties with range segmentation are its character and the absence of a correct segmentation definition. Range segmentation frequently suffers from a significant lack of comparative results and methods [43]. The range image contains information related to the pixel's intensity like the intensity image, but in addition, it contains a vector associated with the range of that pixel "called RANGEL". It provides geometric information about the object independently of the

position, orientation and intensity of the luminous sources illuminating the scene or the reflectance properties of the object [53]. Range image segmentation is similar to the classical 2D image segmentation techniques; we can typically distinguish two classes of methods, edge-based and region-based approaches and possibly hybrid methods implementing the two previous approaches [8].

3 Proposed watermarking scheme

The proposed watermarking scheme consists of two steps, the first one consists in segmenting the image to locate the contour points. Then, the integration process hides the watermark bits in the obtained contour points.

3.1 Pre-processing

Range images are known to be highly noisy, and this makes their segmentation difficult [28], noisy rangels often lead to poor segmentation results and we therefore need to pre-process these images before segmenting them to improve their quality to attenuate the effects of any noise present, the image is filtered by the Floyd & Steinberg filter [16] which improves the global perception of an image and avoids the exclusion of low-intensity areas (Fig. 1). The Floyd-Steinberg algorithm is an example of the error diffusion technique. The objective is to use simple filtering thresholds on each row. This 3×3 matrix screening maintains a great compliance with the nuances. It should be considered that the pixels in the last column of the image do not consider right-hand neighbors and those in the last row do not have any lower neighbors. They are nevertheless modified, specifically by processing the previous column or row. This method is frequently used by web browsers to display color images when there are only 256 colors available.

3.2 Classical active contour segmentation

The classic snake implements a parametric curve C attracted to high gradient areas, where the gradient norm of a point will be high. The principle consists in placing in the image in the

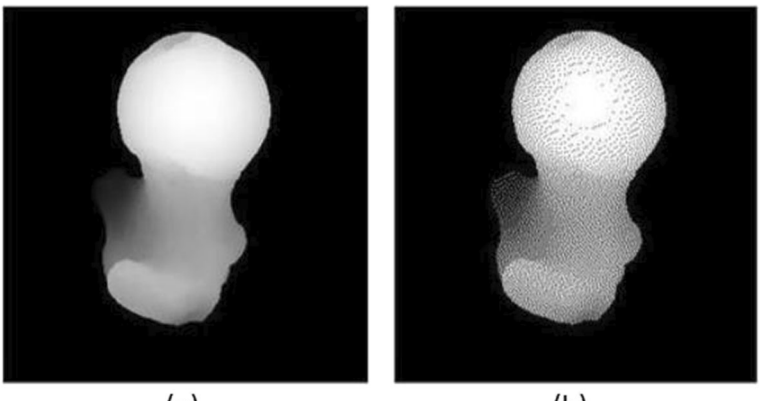

Fig. 1 Watermarking results, **a** Original range image, **b** Filtered image using Floyd & Steinberg

neighborhood of the shape to be detected an initial contour which will then be deformed under the action of several forces. This operation expects a certain amount of energy consisting of internal and external energy. The internal energy will depend on the first and second order derivatives of the parametric curve representing the snake. This energy corresponds to the morphology and characteristics of the curve like curvature, length, this energy is defined by the following function:

$$Eint = \alpha(\mathrm{s})\left(\frac{dv}{ds}\right)^2 + \beta(\mathrm{s})\left(\frac{d^2v}{ds^2}\right)^2 \tag{1}$$

Where α is the elasticity factor β is the rigidity factor of the contour allowing to obtain more or less smooth curves.

External energy refers to the image and its properties and characteristics like the presence of edges or noise [29]. It ensures the snake is at the edges of the image by maximizing the amount of the standard gradient along the curve and so minimizing its opposite, this energy is defined by the following function:

$$Eext = -\gamma(s)|\Delta I\ (v(s))|^2 \tag{2}$$

Where γ depends on the initial image and Δ is the gradient operator. The gradient can be preceded by a low-pass filtering of the image to obtain less noisy contours and increase their influence zone.

The initial contour is first placed in the center of the image in a circle form, the displacement and evolution of this model is done by iteration of the algorithm to minimize the total energy. For each point P of the active contour, the energy function E is calculated for all points n belonging to the neighborhood of P. The point P_0 characterized by the minimum energy E_0 is then chosen to replace P if $E > E_0$, otherwise the contour point P is not modified. This mechanism is rehearsed until convergence (when the contour obtained at iteration t is identical to that obtained at iteration t + 1).

3.3 Adaptive active contour segmentation

The adaptive active contour combines two classic approaches [14], deformable contours and classic active contours. In the formulation of deformable contours, only the normal component of the deformation vector operates on the curve shape. This model is based on the deformation along the normal and makes the snake attracted to the narrowest edges found perpendicular to the model (detecting the contours perpendicular to the model is necessary to enter the cavities). As with the classical active contour approach, the model regulation is achieved by minimizing an internal energy calculated as follows:

$$Eint = \int\left(\alpha(\mathrm{s})\left|v'(s)\right|^2 + \ \beta(\mathrm{s})\left|v''(s)\right|^2\right) ds \tag{3}$$

Where v (s) is the curve, α and β are regularization parameters that vary along the curve. β is fixed to zero to increase the computing speed.

Initially, the contour represents a large circle around all the shapes of the scene. Then, for each iteration, each point P is drawn to the narrowest edge along the normal of that point (edges are detected using the Canny-Deriche operator). Starting from the position of a point P1. Along the normal of this row, the nearest row with gradient amplitude exceeding a specific threshold is searched for, within a specific distance range in both directions. Initially, the regularization parameters are high to ensure the accurate model captures the general shape of the object. At each iteration, the average displacement D of each contour point is calculated an increase of this value from one iteration to the next indicates the snake continues towards the edges and no parameters will be changed, if the distance D decreases, the regularization parameters are decreased for the subsequent iteration. This mechanism allows the snake to gradually enter the cavities. In addition, the smoothing criterion adjusted by the Canny-Deriche operator is also adapted according to the evolution of the snake. Smoothing is important during the first iterations to avoid noise sensitivity, then it is reduced and a new gradient image is computed at each iteration. The final displacement is the result of a compromise between moving completely to the nearest contour along the normal and satisfying geometrical constraints embedded in the internal energy. The algorithm is stopped if no contour point changes position or if the maximum number of iterations is reached.

3.4 Level set

The Level Set technique [47] represents a significant category of modern image segmentation techniques based on PDE partial differential equations, which is a progressive evaluation of the differences between neighbouring pixels to find the contours of objects, ideally, the algorithm converges at the edge of the object where the differences are highest, the noticeable feature of these methods is that the contours can split or merge according to changes in the adjustment function [48]. This method can also detect more than one boundary simultaneously by placing multiple initial contours, but the speed of convergence will be slower than other segmentation methods. A significant challenge in active contours is the correct positioning of the initial contour. Since the contour moves either inward or outward, the resulting segmentation is extremely dependent on the initial location of the contour points. Initially, we start with a closed curve and allow it to move perpendicularly to itself at a prescribed speed. We describe this curve using an explicit parametric (as for the classical active contour). Although this parametric shape is difficult when the curves have to be split or merged, to overcome this problem, when the requested form evolves the implicit active contour takes the original interface and incorporates it into the scalar function of a larger dimension defined throughout the image. The adjustment procedure is a signed distance function, starting from the set zero level it produces a closed curve C_0, if the pixel is on the curve the function is equal to zero, else the function returns the minimum distance between the pixel and the curve (the distance is negative for pixels inside C_0 and positive for pixels outside C_0). This function varies with time and space and evolves using a partial derivative equation (PDE)

$$\omega_{t+1} + F|\nabla\omega_t| = 0 \tag{4}$$

Where F is the speed in the direction of the normal N to the curve, we consider the evolution of the function in a direction perpendicular to itself.

This speed F is composed of three terms, a constant term (like the force of inflation used in deformable models), a dependent term on the local curvature at each location, and a dependent term on the image (in our work, the image's edges).

$$\omega_{n+1} = \omega_n - dt * k_1(x,y) * (Un - \varepsilon K) * |\nabla \omega_n| \quad \varepsilon \in [0,1] \tag{5}$$

Un is the function defining the zone or object to be searched, K the local curvature at each instant t and K_1 the stop criterion.

3.5 Integration process

To integrate the watermark bits, exclusive or is used between the snake pixels, this combination determines which pixel will be modified to satisfy the equalities in Fig. 2.

The modification consists in modifying the parity of the pixel by replacing the least significant bit. This integration scheme allows the integration of two bits by modifying only one of the three pixels used. This will generate less distortion and keep a good similarity between the initial and watermarked image.

3.6 Extraction process

Since the proposed watermarking is blind, the original image is unused for watermark extraction. Floyd & Steinberg's filter is applied to the image to improve the overall perception of an image and avoids the exclusion of low intensity areas. Then, an active contour segmentation is performed on the watermarked image using an active contour, and an adaptive active contour segmentation for watermarked images using an adaptive snake, and a Level set segmentation for watermarked images using Level set. To get the watermark bits, the resulting snake coordinates are then combined using the following formula:

$$X = (S1\%2) \oplus (S3\%2) \text{ and } Y = (S2\%2) \oplus (S3\%2) \tag{6}$$

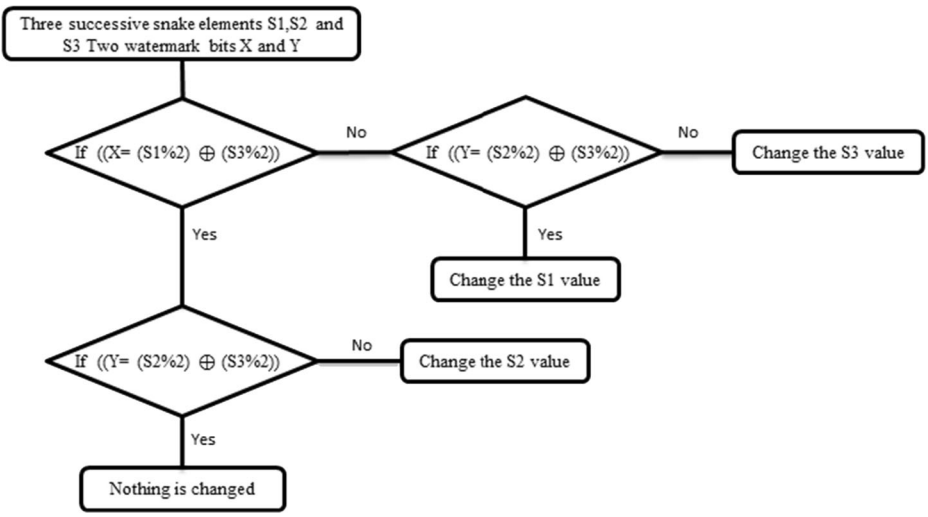

Fig. 2 Substitution rules

4 Experimental results and discussions

To experiment the proposed approach, a range image database from the University of Stuttgart [46] is used. This database contains a collection of synthetic range images taken from high-resolution polygonal models available on the web. Six of these models were reconstructed from real range scans in the Stuttgart lab (07_Deoflach, 08_Deorund, 15_Mole, 24_Kroete, 28_Ente, 29_Schwein).

These images are segmented using the three segmentation algorithms, then the watermark bits are integrated by combining the least significant bits of the obtained snake elements. In the segmentation process, When the snake algorithm achieves a stable state in which no points change positions, it stops. A maximum number of iterations is specified to prevent the search from continuing endlessly. When this number is achieved, the search ends and the current iteration's result is suggested as the final solution (Fig. 3). The calculation time after several executions represent 807 milliseconds on average for the integration process and 542 milliseconds on average for the extraction process.

A visual evaluation (Fig. 4) shows that the segmentation results obtained by the classical snake for range images with cavities are not complete and this shows the limits of the classical active contour. The traditional snake does not converge correctly towards the concavities. The model converged before some elements of the active contour could reach some edges of the shape. The adaptive snake, on the other hand, offers very good segmentation results even for images with cavities. The regularization parameters allow the snake to gradually enter the cavities. The smoothing parameter is adjusted by the Canny-Deriche operator is also adapted according to the evolution of the snake. To evaluate the three segmentation algorithms, Good Segmentation Rates (GSR) was calculated for all three algorithms. As we can see in Table 1, the classical active contour algorithm offers a good GSR for simple images without a cavity; however, for images with a cavity, the results of the adaptive active contour and the level set are significantly better. Since the contour points obtained represent the integration space of the watermark, the capacity of the watermarking process is variable and depends on the contour obtained. The larger the contour of the shape the more contour points will be and therefore increase the integration capacity. As we can see in Table 1, the adaptive active contour offers the most reasonable compromise between good segmentation rate/Snake elements, this algorithm allows to generate an adequate number of snake elements (SE) while offering a good segmentation rate for simple images as well as images with the cavity.

4.1 Imperceptibility test

After the watermark integration, it can be seen in Fig. 5 that the two images are visually similar. Therefore, to evaluate the imperceptibility of our approach, objective evaluation measurements are used. We will therefore calculate the PSNR (Peak Signal to Noise Ratio), which allows us to measure the distortions generated by the integration process [40], as well as the Structural Similarity (SSIM), which is regularly used to measure the similarity between two images [18]. The number of values modified by the integration process (Number of Changing Pixel Rate), as well as the UACI (Unified Averaged Changed Intensity) is also calculated.

In such a working environment as watermarking digital images, where we seek that the scheme must be robust and imperceptible and meet the requirements and constraints solicited by the efficient watermarking systems. Quantitative distortion measures are much more

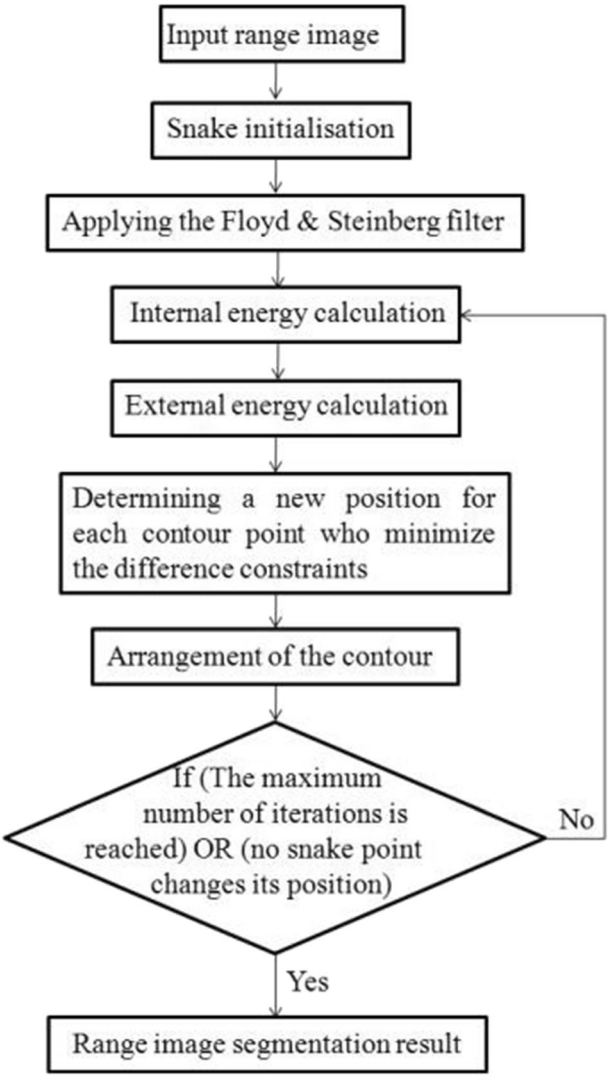

Fig. 3 Range segmentation process

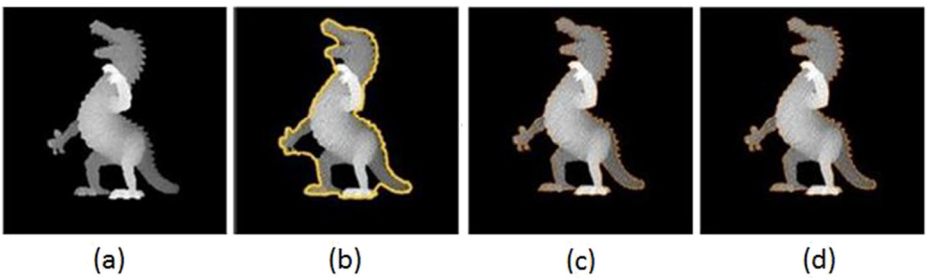

Fig. 4 Segmentation results, **a** Original image, **b** segmentation using active contour, **c** segmentation using adaptive contour, **d** segmentation using Level set

Table 1 Segmentation results

	Images without cavity		Images with cavity		Overall result	
	SE	RGS	SE	RGS	SE	RGS
Classique snake	4526	99.19%	8498	76.48%	6589	75.07%
Adaptive snake	5029	95.18%	5828	96.16%	5828	84.74%
Level set	4194	94.24%	4935	94.67%	5908	93.89%

efficient and allow a valid comparison between the various methods compared to subjective assessment measures.

Peak signal to noise ratio The most popular distortion measure in image processing is the Peak Signal to Noise Ratio [6]. It is defined by the following formula:

$$(PSNR)_{dB} = 10\ log_{10}\ \left[\mathrm{M*N}\frac{\max \mathrm{I}^2(\mathrm{i},\mathrm{j})}{\sum \mathrm{i},\mathrm{j}\ [\ \mathrm{I}(\mathrm{i},\mathrm{j})-\mathrm{J}\ (\mathrm{i},\mathrm{j})]^2}\right. \tag{7}$$

Where I (i, j) is the value of the luminance of the reference pixel (i, j) and J (i, j) that of the image to be tested, the two images being of size [M × N].

Structural similarity index (SSIM) Another criterion for measuring similarity is the SSIM [13] which is used regularly to measure the similarity between two proposed images. It is defined as follows:

$$SSIM(x,y) = \frac{\left(2\mu_x\mu_y + C_1\right)\left(2\delta_{xy} + C_2\right)}{\left(\mu_x^2 + \mu_y^2 + C_1\right)\left(\delta_x^2 + \delta_y^2 + C_2\right)} \tag{8}$$

Where: μ_x- Average of x. μ_y- average of y. δ_x^2- variance of x. δ_y^2- variance of y. δ_{xy}- covariance of x y.

C1=k1L2-Constant to avoid instability when $\mu_x^2 + \mu_y^2$ is close to zero; k1 = 0.01, =255.

C2=k2L2- Constant to avoid instability when $\delta_x^2 + \delta_y^2$ is close to zero; k2 = 0.03, =255.

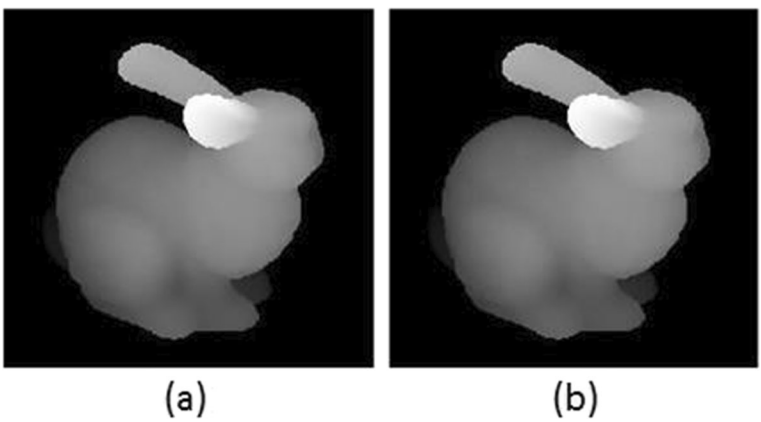

Fig. 5 Watermarking results, **a** Original image, **b** Watermarked image

Mean squared error The MSE measures the average term difference between the original image and the output one (the watermarked image). The larger the MSE the higher the level of degradation [44]. The MSE is defined by the following formula:

$$MSE = \frac{1}{\mathrm{M}*\mathrm{N}} \sum_i \sum_j (I(i,j) - J(i,j))^2 \tag{9}$$

Where I (i, j) is the value of the luminance of the reference pixel (i, j) and J (i, j) that of the image to be tested, the two images being of size [M × N].

The number of changing pixel rate The NCPR parameter [38] calculates the rate of change of pixels in the watermarked image ($\mathbf{CI_2}$) obtained by comparing it to the original image ($\mathbf{CI_1}$). The two images being of size [M × N]. It can be calculated using the following formula:

$$NPCR = \sum_{i=1}^{M} \sum_{j=1}^{N} \frac{D(i,j)}{T} * 100\% \tag{10}$$

$$D(i,j) = \begin{cases} 0, & if\ CI_1(i,j) = CI_2(i,j) \\ 1, & if\ CI_1(i,j) \neq CI_2(i,j) \end{cases} \tag{11}$$

The unified averaged changed intensity The average rate of intensity change [7] is analyzed using the UACI parameter by comparing the original image ($\mathbf{CI_1}$) and the watermarked image ($\mathbf{CI_2}$). The two images being of size [M × N]. The UACI is defined by the following formula:

$$UACI = \sum_{i=1}^{M} \sum_{j=1}^{N} \frac{CI_1(i,j) - CI_2(i,j)}{F*T} * 100\% \tag{12}$$

Where F is the largest pixel value supported by the image format.

The similarity and distortion results obtained are almost similar for the three algorithms since the integration process is the same. The unique difference remains the location of the modified pixels, which depends on the snake elements obtained by the segmentation process. We can conclude from the results obtained that the integration process offers a good imperceptibility rate with PSNR >66 dB as well as a good structural similarity between the initial and watermarked image. This is justified by the slight amount of data modified by the integration process, in fact, the modification of a single LSB for the integration of two bits of the watermark allows to generate a watermarked image more similar to the original image Table 2.

4.2 Robustness test

In order to evaluate the robustness of the watermark, the normalized correlation is calculated using the original mark and the extracted mark [51]. This coefficient is used to evaluate the existence and accuracy of the extracted mark. This correlation is calculated by the following formula:

Table 2 Imperceptibility results

	PSNR	MSE	SSIM	NCPR	UACI
Classique snake	66,60	0.03190	0.9999	0,0318	0,00012
Adaptive snake	66,04	0.02123	0.9997	0,0210	0,00008
Level set	66,72	0.03197	0.9998	0,0318	0,00012

$$NC = \frac{\sum_{i=1}^{n}\sum_{j=1}^{m} M(i,j) * N(i,j)}{\sum_{i=1}^{n}\sum_{j=1}^{m} M(i,j)^2} \tag{13}$$

Where M and N are respectively the original and the extracted mark of sizes i * j.

A watermark is generally considered to be robust for normalized cross-correlation in image watermarking NCC $\geq$ 0.75. The BER (Bit Error Ratio) is also calculated to evaluate the similarity between the two watermarks, the inserted and the extracted watermark [41]. Bit Error Rate determines the number of errors occurring between the original and the extracted watermark, it is calculated as follows:

$$\text{BER} = \frac{\text{nomber of errors}}{\text{number of watermark bits}} \tag{14}$$

The value tending towards zero means that the watermarking maintains an adequate reliability (the extracted mark is almost similar to the detected mark). As we can see in Table 3, the normalized cross-correlation rate obtained by watermarking using the classical active contour is significantly lower than the results obtained by the other two algorithms. This is explained by the poor segmentation results of cavity images. Unlike the contour points which are static, the snake points are dynamic and the segmentation obtained can vary according to the iterations and parameters used which can generate a various snake at each execution and therefore lose the location of the watermarked pixels. The extraction process is therefore closely linked to the segmentation performed; a good segmentation allows recovering all the watermarked pixels. As we can see in Table 3, the watermark embedded in the contour points generated by the adaptive active contour and the Level sets are resistant to the various attacks of noise addition, filtering, Scaling or Sharpening but are vulnerable to compression attacks. Which is frequent in spatial watermarking techniques.

Table 3 Robustness results

	Classique snake		Adaptive snake		Level set	
	NCC	BER	NCC	BER	NCC	BER
Without attacks	0,7139	0,0318	0,9727	0,0011	0,9253	0,0013
Histogram equalization	0,7451	0,0222	0,9736	0,0015	0,8772	0,0019
Gaussian noise	0,6418	0,0139	0,9614	0,0149	0,9692	0,0091
Salt & Pepper Noise	0,7203	0,0356	0,9878	0,0178	0,8622	0,0267
Average filtering	0,8647	0,0276	0,9623	0,0125	0,9641	0,0079
JPEG compression	0,6353	0,0356	0,7505	0,0366	0,7891	0,0381
Cropping	0,6883	0,0229	0,9205	0,0129	0,8963	0,0142
Scaling	0,7454	0,0412	0,9678	0,0153	0,9510	0,0139
Sharpening	0,7115	0,0220	0,9114	0,0277	0,8365	0,0225

5 Conclusion

Because of the illicit uses of digital documents, digital watermarking has been introduced as an effective technique for copyright protection, copy protection or digital image authenticity. In this work we have presented a watermarking approach for range image protection. In this approach, the watermark is integrated into the active contour elements obtained after segmentation. For this, an active contour is applied to the image and then the watermark bits are substituted for the least significant bit of the pixels corresponding to the active contour elements. Although the active contour is inappropriate for range segmentation since it generates a contour whereas range segmentation should generate a volume, in our approach only the contour is needed for the watermark integration. In this work we used three types of active contour for segmentation, a classical active contour, an adaptive active contour and a level set active contour. The Snakes approach the narrowest local minimum of the initial contour and are therefore prone to providing a local minimum which in general does not coincide with the object contour. This leads to sensitivity to initialization, for example when there are a high number of local minima near the initial contour due to image noise or background clutter. The discretization of the contours into a number of control points may cause problems with uneven spacing and self-crossing while the contours are deforming and make it difficult to extend the approach to segment 3D objects. The automatic selection of various parameters like the weights in the energy function remains an evident problem. We can conclude from the obtained segmentation results that the adaptive active contour and the level set offer a good compromise between the rate of good segmentation and the number of Snake elements, contrary to the classical active contour which does not converge correctly towards the cavities. Imperceptibility tests confirm that the proposed integration process offers a good imperceptibility rate as well as a good structural similarity between the initial and watermarked image. The robustness tests have shown the watermark is resistant to several attacks commonly used in image watermarking like noise addition or filtering however, the proposed approach is vulnerable to compression attacks. The integration in the transform domain could overcome this limitation since the use of transforms allows generating a watermarked image more robust to compression attacks.

Acknowledgments This work was supported by " La Direction Générale de la Recherche Scientifique et du Développement Technologique (DGRSDT)" of Algeria.

Data availability The data used to support the findings of this study could be found freely here: http://range.informatik.uni-stuttgart.de/htdocs/html /.

Declarations

Conflict of interest The authors declare that they have no known competing financial interests or personal relationships that could have appeared to influence the work reported in this paper.

Ethical approval This article does not contain any studies with human participants or animals performed by any of the authors.

References

1. Abdallah EE, Hamza AB, Bhattacharya P (2007) MPEG video watermarking using tensor singular value decomposition. In: Image analysis and recognition, Berlin, Heidelberg, p. 772-783. https://doi.org/10.1007/978-3-540-74260-9_69
2. Abdallah EE, Hamza AB, Bhattacharya P (2007) Spectral graph-theoretic approach to 3D Mesh watermarking. In: Proceedings of Graphics Interface 2007, New York, NY, USA, p. 327-334. https://doi.org/10.1145/1268517.1268570.
3. Abdallah EE, Hamza AB, Bhattacharya P (2008) Robust 3D watermarking technique using Eigendecomposition and nonnegative matrix factorization. In: Image analysis and recognition, Berlin, Heidelberg, p. 253-262. https://doi.org/10.1007/978-3-540-69812-8_25
4. Abdallah EE, Ben Hamza A, Bhattacharya P (2008) Watermarking 3D models using spectral mesh compression. SIViP 3(4):375. https://doi.org/10.1007/s11760-008-0079-y
5. Abdallah EE, Ben Hamza A, Bhattacharya P (2010) Video watermarking using wavelet transform and tensor algebra. SIViP 4(2):233–245. https://doi.org/10.1007/s11760-009-0114-7
6. Ahmadi S, Zhang G, Wei S, Boukela L (2020) An intelligent and blind image watermarking scheme based on hybrid SVD transforms using human visual system characteristics. Vis Comput 37(2):385–409
7. Ahmadi S, Zhang G, Wei S (2020) Robust and hybrid SVD-based image watermarking schemes: a survey. Multimed Tools Appl 79:1075–1117
8. Amine K, Farida MH (2015) Quantitative comparison of deformable models in range segmentation. Cybern Inf Technol 14(4):66–79. https://doi.org/10.1515/cait-2014-0006
9. Amine K, Fares K, Redouane KM, Salah E (2022) Medical image watermarking for telemedicine application security. J Circuit Syst Comp 31(05):2250097. https://doi.org/10.1142/S0218126622500979
10. Aparna P, Kishore PVV (2018) Bio -metric based efficient medical image watermarking in ehealthcare application. IET Image Process 13:421–428
11. Aparna P, Kishore PVV (2019) Biometric-based efficient medical image watermarking in E-healthcare application. IET Image Process 13:421–428
12. Barania M, Peyman A, Valandar M, Irani B (2020) A blind video watermarking algorithm robust to lossy video compression attacks based on generalized Newton complex map and contourlet transform. Multimed Tools Appl 79:2127–2159
13. Barania M, Peyman A, Valandar M, Irani B (2020) A new Pseudo random number generator based on generalized Newton complex map with dynamic key. J Inf Secur Appl 53:102509
14. Braiki M, Benzinou A, Nasreddine K, Hymery N (2020) Automatic human dendritic cells segmentation using K-means clustering and Chan-Vese active contour model. Comput Methods Prog Biomed 195:105520
15. Chauhan DS, Singh AK, Kumar B, Saini JP (2019) Quantization based multiple medical information watermarking for secure e-health. Multimed Tools Appl 78:3911–3923
16. Duan Y, Peng T, Qi X (2020) Active contour model based on LIF model and optimal DoG operator energy for image segmentation. Optik 202:163667
17. Fares K, Amine K, Salah E (2020) A robust blind color image watermarking based on Fourier transform domain. Optik 208:164562. https://doi.org/10.1016/j.ijleo.2020.164562
18. Fares K, Khaldi A, Redouane K, Salah E (2021) DCT & DWT based watermarking scheme for medical information security. Biomed Signal Process Control 66:102403. https://doi.org/10.1016/j.bspc.2020.102403
19. Galdames F, Claudio A, Pablo A, Martin A (2019) Rock lithological classification by hyperspectral, range 3D and color images. Chemom Intell Lab Syst 189:138–148
20. Haddad S, Coatrieux G, Moreau-Gaudry A, Cozic M (2020) Joint watermarking-encryption-JPEG-LS for medical image reliability control in encrypted and compressed domains. IEEE Trans Inf Forensic Secur 15:2556–2569
21. Hassan B, Ahmed R, Li B, Hassan O (2019) An imperceptible medical image watermarking framework for automated diagnosis of retinal pathologies in an eHealth arrangement. IEEE Access 7:69758–69775
22. Holz D, Behnke S (2014) Approximate triangulation and region growing for efficient segmentation and smoothing of range images. Robot Auton Syst 62:1282–1293
23. Hsu L, Hu H (2019) A reinforced blind color image watermarking scheme based on Schur decomposition. IEEE Access 7:2169–3536
24. Kahlessenane F, Khaldi A, Kafi MR, Euschi S (2021) A color value differentiation scheme for blind digital image watermarking. Multimed Tools Appl 80(13):19827–19844. https://doi.org/10.1007/s11042-021-10713-6
25. Kahlessenane F, Khaldi A, Kafi R, Euschi S (2021) A robust blind medical image watermarking approach for telemedicine applications. Clust Comput 24(3):2069–2082. https://doi.org/10.1007/s10586-020-03215-x

26. Kahlessenane F, Khaldi A, Kafi R, Euschi S (2021) A DWT based watermarking approach for medical image protection. J Ambient Intell Humaniz Comput 12(2):2931–2938. https://doi.org/10.1007/s12652-020-02450-9
27. Kahlessenane F, Khaldi A, Kafi MR, Zermi N, Euschi S (2021) A value parity combination based scheme for retinal images watermarking. Opt Quant Electron 53(3):161. https://doi.org/10.1007/s11082-021-02793-3
28. Khaldi A, Merouani H (2012) An active contour for range image segmentation, Signal & Image Processing: an. Int J 03:17–29
29. Khaldi A, Merouani H (2014) An deformable models approach for range image segmentation. Int J Imaging Robot 12:39–48
30. Khaldi A, Kafi MR, Moad MS (2022) Wrapping based curvelet transform approach for ECG watermarking in telemedicine application. Biomed Signal Process Control 75:103540. https://doi.org/10.1016/j.bspc.2022.103540
31. Lee BR, Hamza AB, Krim H (2002) An active contour model for image segmentation: A variational perspective. In: 2002 IEEE International Conference on Acoustics, Speech, and Signal Processing, vol. 2, p. II-1585-II-1588. https://doi.org/10.1109/ICASSP.2002.5744919.
32. Lee YS, Seo YH, Kim DW (2019) Digital blind watermarking based on depth variation prediction map and DWT for DIBR free-viewpoint image. Signal Process Image Commun 70:104–113
33. Liu Y, Zhang S, Yang J (2020) Color image watermark decoder by modeling quaternion polar harmonic transform with BKF distribution. Signal Process Image Commun 88:115946
34. Mlynarskia P, Delingettea H, Criminisib A, Ayachea N (2019) 3D convolutional neural networks for tumor segmentation using long-range 2D context. Comput Med Imaging Graph 73:60–72
35. Moad MS, Kafi MR, Khaldi A (2022) A non-subsampled Shearlet transform based approach for heartbeat sound watermarking. Biomed Signal Process Control 71:103114. https://doi.org/10.1016/j.bspc.2021.103114
36. Moad MS, Kafi MR, Khaldi A (2022) Medical image watermarking for secure e-healthcare applications. Multimed Tools Appl. https://doi.org/10.1007/s11042-022-12004-0
37. Moad MS, Kafi MR, Khaldi A (2022) A wavelet based medical image watermarking scheme for secure transmission in telemedicine applications. Microprocess Microsyst 90:104490. https://doi.org/10.1016/j.micpro.2022.104490
38. Mothi R, Karthikeyan M (2019) Protection of bio medical iris image using watermarking and cryptography with WPT. Measurement 136:67–73
39. Najafi E, Loukhaoukha K (2019) Hybrid secure and robust image watermarking scheme based on SVD and sharp frequency localized contourlet transform. J Inf Secur Appl 44:144–156
40. Nuñez-Ramirez D, Cedillo-Hernandez M, Nakano-Miyatake M, Perez-Meana H (2020) Efficient Management of Ultrasound Images using digital watermarking. IEEE Lat Am Trans 18:1398–1406
41. Peyman A, Setayeshib S, Rahmanic A (2020) Deterministic chaos game: a new fractal based pseudo-random number generator and its cryptographic application. J Inf Secur Appl 52:102472
42. Prasetyo H, Hsia C, Liu C (2020) Vulnerability attacks of SVD-based video watermarking scheme in an IoT environment. IEEE Access 8:69919–69936
43. Salah E, Amine K, Redouane KM, Fares K (2021) Spatial and frequency approaches for audio file protection. J Circuit Syst Comp 30(12):2150210. https://doi.org/10.1142/S0218126621502108
44. Salah E, Amine K, Redouane K, Fares K (2021) A Fourier transform based audio watermarking algorithm. Appl Acoust 172:107652. https://doi.org/10.1016/j.apacoust.2020.107652
45. Sayah MM, Redouane KM, Amine K (2022) Secure transmission and integrity verification for color medical images in telemedicine applications. Multimed Tools Appl. https://doi.org/10.1007/s11042-021-11791-2
46. The University of Stuttgart (2001) Stuttgart range image database. http://range.informatik.uni-stuttgart.de/htdocs/html/.
47. Yang Y, Wang R, Feng C (2020) Level set formulation for automatic medical image segmentation based on fuzzy clustering. Signal Process Image Commun 87:115907
48. Yang Y, Feng C, Wang R (2020) Automatic segmentation model combining U-net and level set method for medical images. Expert Syst Appl 153:113419
49. Zermi N, Khaldi A, Kafi MR, Kahlessenane F, Euschi S (2021) A lossless DWT-SVD domain watermarking for medical information security. Multimed Tools Appl 80(16):24823–24841. https://doi.org/10.1007/s11042-021-10712-7
50. Zermi N, Khaldi A, Kafi MR, Kahlessenane F, Euschi S (2021) Robust SVD-based schemes for medical image watermarking. Microprocess Microsyst 84:104134. https://doi.org/10.1016/j.micpro.2021.104134

51. Zermi N, Khaldi A, Kafi R, Kahlessenane F, Euschi S (2021) A DWT-SVD based robust digital watermarking for medical image security. Forensic Sci Int 320:110691. https://doi.org/10.1016/j.forsciint.2021.110691
52. Zermi N, Khaldi A, Kafi MR, Kahlessenane F, Euschi S (2022) An SVD values ordering scheme for medical image watermarking. Cybern Syst 53(3):282–297. https://doi.org/10.1080/01969722.2021.1983700
53. Zhou S, Song W (2020) Deep learning-based roadway crack classification using laser-scanned range images: a comparative study on hyperparameter selection. Autom Constr 114:103171